Available online at www.sciencedirect.com
ScienceDirect
Journal of Power Sources 158 (2006) 1313–1316
JOURNAL OF POWER SOURCES
www.elsevier.com/locate/jpowsour

Short communication

Improving the stability of direct-methane solid oxide fuel cells using anode barrier layers

Yuanbo Lin, Zhongliang Zhan, Scott A. Barnett *

Department of Materials Science and Engineering, 2220 Campus Drive, Northwestern University, Evanston, IL 60208, USA

Received 5 July 2005; received in revised form 20 September 2005; accepted 24 September 2005
Available online 14 February 2006

Abstract

Solid oxide fuel cells (SOFCs) were characterized with methane as the fuel, both with and without an inert porous layer placed between the anode and the fuel stream. For a given set of operating conditions, SOFCs were stable without coking above a critical current density. The barrier layer decreased the critical current density, e.g. from 1.8 to <0.6 A cm^{-2} at 800 °C. This much-increased stable operating range is discussed in terms of mass transport through the barrier layer.

Keywords: Solid oxide fuel cell (SOFCs); Direct methane operation; Ni-YSZ anode-supported; Internal reforming

Direct-methane solid oxide fuel cells (SOFCs) are of interest as a potentially simple means of electrical generation from natural gas [1], and also for syngas and electricity co-generation by electrochemical partial oxidation [2,3]. There have been numerous reports of stable direct-methane SOFC operation, many of which utilized Ni-based anodes [4–7]. This is despite the well-known tendency of Ni to coke when exposed to hydrocarbons [8]. Recent studies suggest two main explanations for this apparent discrepancy. First, for SOFCs working at temperatures <700 °C, the methane pyrolysis kinetics on Ni are relatively slow [9]. Second, SOFC reaction products help suppress coking [10]. This latter point was based on the observation that stable coke-free operation was achieved for SOFC current density above a critical value. The mechanism proposed was that H_2O and CO_2 electrochemical products help remove solid carbon and/or reduce the methane partial pressure (and hence reduce coking) via reforming. However, the rate of reaction product formation at critical current, relative to the methane flow rate, was much too small to explain the non-coking results. The results were thus explained by concentration of reaction products and dilution of methane within the anode due to mass transport limitations.

Fig. 1a shows schematically the expected methane and reaction product concentrations in the near-anode region during direct-methane SOFC operation [10]. A gas diffusion limitation within the thick Ni-based anode support is assumed [11], giving rise to a decrease in methane content, and an increase in the product content, going from the free anode surface to the electrolyte. That is, coking should be less favorable near the electrolyte than near the free surface. This proposed mechanism was supported by SEM-EDX measurements showing no coking near the electrolyte even when it was observed near the free surface [10]. Indeed, examination of Fig. 1a suggests that gas diffusion gradients will have little effect on coking conditions near the anode free surface, since the diffusivity across the stagnant layer at the anode surface is relatively high.

Here, we have tested the above theory by adding an inert, non-coking porous layer, i.e. a diffusion barrier, to the anode. As illustrated in Fig. 1b, this should reduce coking via a decrease in methane and increase in product concentrations throughout the anode. Life tests were used to observe cell stability under different operating conditions, and post-test observations were used to observe any carbon deposition.

The Ni-YSZ anode-supported fuel cells were prepared as follows. Ni-YSZ anode supports were made by mixing NiO (Baker) and 8-YSZ (Tosoh), in a weight ratio of 1:1, and ball milling in ethanol for about 20 h. Starch (10 wt.%) was then added to the mixture and the ball milling was continued for another 2 h. The milled powder mixture was dried and pressed into pellets with diameter of 19 mm and thickness of about 0.7 mm. The pellets were bisque fired at 1000 °C for 4 h. A YSZ electrolyte layer

* Corresponding author. Tel.: +1 847 491 2447; fax: +1 847 491 7820.
E-mail address: s-barnett@northwestern.edu (S.A. Barnett).

0378-7753/$ – see front matter © 2005 Elsevier B.V. All rights reserved.
doi:10.1016/j.jpowsour.2005.09.060

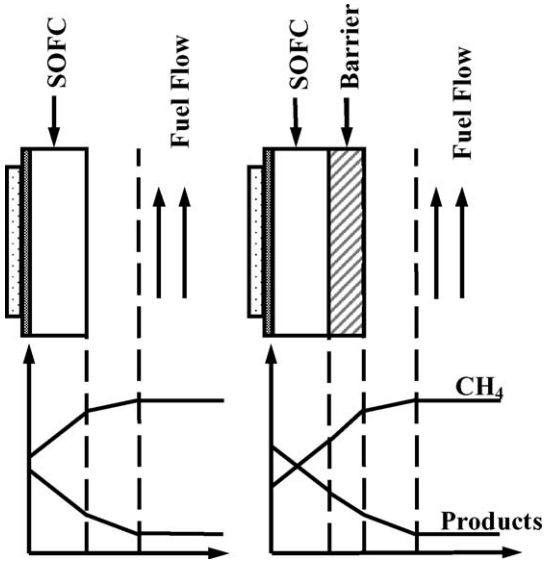

Fig. 1. Simplified schematic illustrations of how reactant and product gas concentrations are expected to vary with position during SOFC operation without (left) and with (right) barrier layers.

was colloidally deposited on the anode support and the resulting bi-layer co-sintered at 1400 °C for 4 h. Cathodes consisting of a layer of 70 wt.% $La_{0.6}Sr_{0.4}Fe_{0.2}Co_{0.8}O_3$ (LSCF, Praxair) and 30 wt.% Gd-doped Ceria (GDC, NexTech), followed by pure LSCF layer, were applied by screen printing on the YSZ electrolyte and fired at 900 °C for 4 h.

Barrier layer pellets were composed of partially stabilized zirconia (PSZ) and CeO_2 with the weight ratio of 1:1. Zirconia and CeO_2 are both resistant to coking [12,13]. Pure PSZ layers were also used with similar results. The powders were mixed with 20 wt.% starch filler in ethanol for 20 h. The dried mixed powder was pressed into pellets ≈0.4 mm thick and fired at 1400 °C for 4 h. The porosity as measured by the Archimedes method was 47–49%.

SOFC tests were carried out using a standard testing geometry [10], both with and without barrier layers that were placed directly against the SOFC anodes. The anodes were reduced in humidified hydrogen at 700 °C for several hours and the cell operated in hydrogen for more than 24 h, at which time stable cell characteristics were realized. Current–voltage curves were then taken from 600 to 800 °C using an Electrochemical Workstation (IM6, ZAHNER), with the cathode exposed to ambient air and the anode to humidified (3% H_2O) hydrogen. Current–voltage curves were then recorded with methane as the fuel, taking care to limit the measurement times at low currents and high temperatures, as these conditions yielded coking that degraded the cells [10]. Life tests were done with a methane flow rate of 30 sccm.

The SOFC stability region was determined by the following protocol. First, the fuel was switched from H_2 to methane with the cell maintained near the maximum power point. After the switch to methane, the V value at constant current density J typically dropped by ≈20% to a new steady-state value [10]. Second, J was maintained constant near the maximum power point for >3 h, long enough to observe whether V was stable. Third, J was reduced and maintained constant for >3 h. This latter step was repeated until V became unstable.

Fig. 2 shows results obtained in this way at 800 °C. As shown in Fig. 2a (no barrier), the cell was fully stable in methane only at relatively large current densities, i.e. 1.8 A cm^{-2} at 800 °C. For smaller J, V decreased continuously with time. Subsequent observation of the anodes after degradation showed clear coking, as reported previously [10]. With a barrier layer (Fig. 2b), V remained stable at current densities down to at least ≈0.6 A cm^{-2}. Similar results were observed for a number of similar cells, and slight degradation was typically observed during cell operation at $J < 0.6$ A cm^{-2}. The test shown in Fig. 2b was stopped at 0.6 A cm^{-2}, however, in order to allow evaluation of the anode after stable operation. Longer-term life testing of a cell with barrier layer operated at $J = 0.6$ A cm^{-2} and 750 °C for ∼155 h is shown in Fig. 3. Visual observation and SEM-EDX evaluation after this cell test showed no evidence of coke or structure degradation, on either the barrier layer or anode. This suggests that the barrier layer prevented coking rather than just slowing the process. Overall, these results showed an expanded stable and non-coking cell operation range with the barrier layer.

Fig. 4 provides a direct comparison of SOFC stability with and without barriers at 750 and 800 °C, all at $J = 1$ A cm^{-2}. Again, the voltage was stable with the barriers, but decreased continuously without the barriers. The initial voltage was ≈10% lower with the barrier, presumably a result of the increased gas diffusion polarization. The barriers were also tested at 700 °C,

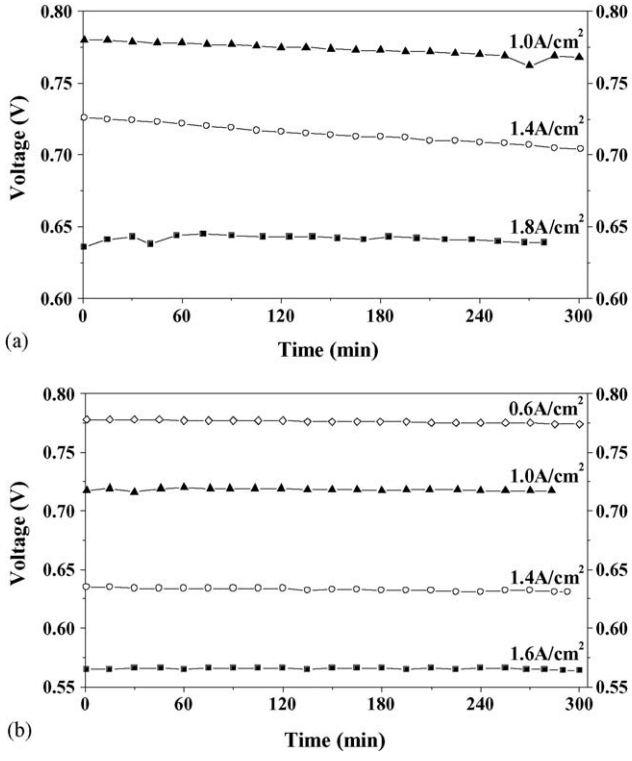

Fig. 2. Cell voltage vs. time at constant current J for SOFCs operated in humidified methane at 800 °C without (a) and with (b) barrier layer. The cells were operated at different J values for 6 h in each step, starting at high J and reducing J in steps.

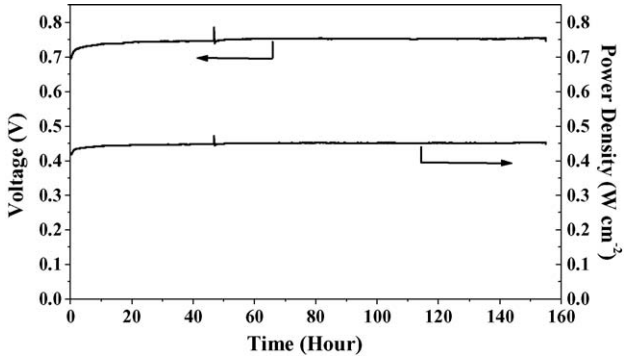

Fig. 3. Voltage and power density vs. time for a SOFC with barrier operated in humidified methane at 750 °C and 0.6 A cm^{-2} with barrier for ∼155 h.

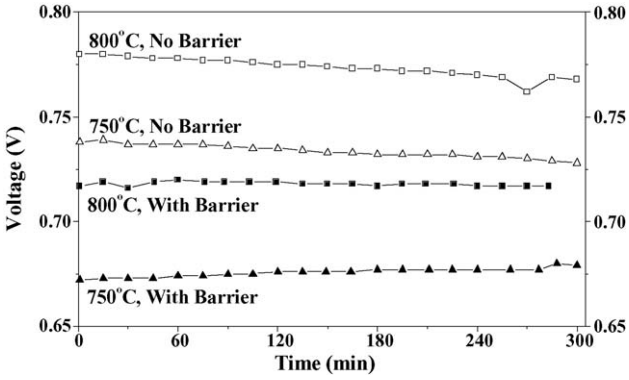

Fig. 4. Cell voltage vs. time at a constant current density $J = 1$ A cm^{-2} for SOFCs operated in humidified methane at 750 and 800 °C with (solid dots) and without (open dots) barrier.

but the critical current densities were already <0.2 A cm^{-2} at this temperature [10], making it difficult to discern the barrier layer effect.

Fig. 5 shows typical voltage V versus current density J of SOFCs with and without a barrier layer operated on 30 sccm humidified methane. Open circuit voltages were lower with the barrier layers, but it should be noted that these were measured during ∼3 s current interruptions (in order to avoid coking), and a steady-state value was not achieved. Limiting current behavior was observed in all cases, but with lower limiting currents with

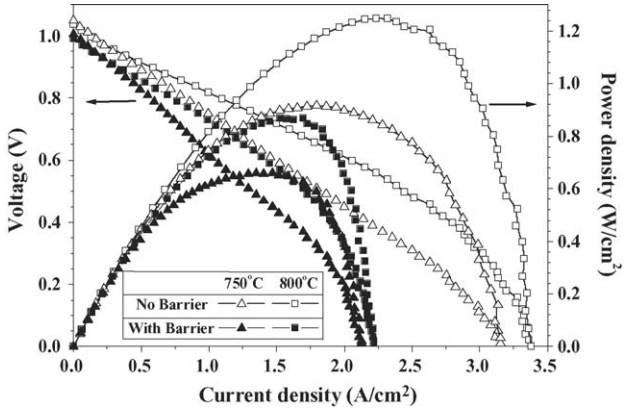

Fig. 5. Voltage vs. current density of SOFCs with (solid dots) and without (open dots) barrier layer operated on 30 sccm humidified methane at 750 and 800 °C.

a barrier layer. This is another indication of an increased gas diffusion limitation caused by the barrier, as suggested in Fig. 1b. The power densities at 0.7 V at 800 °C were 1.0 W cm^{-2} without a barrier layer and 0.8 W cm^{-2} with a barrier layer. For these barrier layers, there was thus an ≈20% power density penalty at a practical SOFC operating point, due to increased concentration polarization.

Barrier layers could be considered as a practical means for making direct methane SOFC stacks more stable against coking. Overall, the present barriers appear to be a reasonable compromise, providing a substantial stability improvement with a small power density penalty. Thinner or more porous barriers could be used to reduce the power density penalty, but this will reduce the effectiveness for suppressing coke formation. It may be useful to vary the barrier layer diffusion resistance versus position in a stack, e.g. using a thicker or less porous barrier near the fuel inlet where coking is most likely, and then reducing and eventually eliminating the barrier downstream where coking is unlikely (i.e. the methane content is reduced and product concentrations large).

We do not believe that the specific material chosen for the diffusion barrier was important—rather, it acted as an inert diffusion-limiting layer. The methane steam reforming catalytic activity of zirconia-ceria diffusion barriers was tested with a micro-channel reactor at different gas composition at 750 and 800 °C. Table 1 shows the experimental conditions and results. There was little or no activity for CeO_2 or doped CeO_2 based materials at such high temperatures, consistent with prior reports [8,9]. However, barrier layers containing a non-coking reforming catalyst, e.g. Ru [14] or Ru-containing perovskites [15], may be useful to further improve anode stability by reforming methane with product molecules before reaching the Ni-based anode. This approach was recently used successfully for *iso*-octane internal reforming SOFCs [14].

In summary, the present results demonstrate that diffusion barrier layers increase the stable operating parameter range of Ni-YSZ anode-supported SOFCs operating directly with methane. At 800 °C, for example, the current density needed for coke-free operation was reduced by a factor of 3. These results are consistent with the simple model wherein the diffusion barrier concentrated reaction products and reduced the methane concentration within the anode (Fig. 1).

Table 1
Steam reforming activity of barrier layer materials

Temperature (°C)	Catalytic activity (methane conversion rate %)	
	Testing series I[a]	Testing series II[b]
750	0.64	0.71
800	0.99	1.6

[a] Gas hourly space velocity (GHSV) = 136.06 k (h^{-1}), gas composition of traditional steam reforming reaction with steam to methane to hydrogen ratio: S/C/H = 3/l/l.

[b] Gas hourly space velocity (GHSV) = 68.56 k (h^{-1}), gas compositions simulate that of a fuel cell working at 2.12 A cm^{-2} with 30 sccm humidified methane (3% steam). Equivalent steam to methane to hydrogen ratio is: S/C/H = 1/3.62/0.

Acknowledgements

The authors gratefully acknowledge the financial support of the Department of Energy SECA Program during this work. Brian Madsen and Tammy Lai, Paul Von Dollen are also acknowledged for their assistance with the experiments. Special thanks to Dr. David King, Pacific Northwest National Laboratory, for the kind help in the catalytic activity measurements.

References

[1] S.A. Barnett, in: W. Vielstich, A. Lamm, H. Gasteiger (Eds.), Handbook of Fuel Cell Technology IV, Fundamentals of Technology and Applications, Wiley, San Francisco, 2003, p. 1098.
[2] V.V. Galvita, V.D. Belyaev, A.K. Demin, V.A. Sobyamin, Appl. Catal. A: Gen. 165 (1997) 301.
[3] G.L. Semin, V.D. Belyaev, A.K. Demin, V.A. Sobyanin, Appl. Catal. A: Gen. 181 (1999) 131.
[4] J. Liu, S.A. Barnett, Solid State Ionics 158 (2003) 11.
[5] A. Weber, B. Sauer, A.C. Muller, D. Herbstritt, E. Ivers-Tiffee, Solid State Ionics 152/153 (2002) 543.
[6] J.B. Wang, J.-C. Jang, T.-J. Huang, J. Power Sources 122 (2003) 122.
[7] C. Xia, F. Chen, M. Liu, Electrochem. Solid State Lett. 4 (2001) A52.
[8] M.L. Toebes, J.H. Bitter, A. Jos van Dillen, K.P. de Jong, Catal. Today 76 (2002) 33.
[9] C.M. Finnerty, N.J. Coe, R.H. Cunningham, R.M. Ormerod, Catal. Today 46 (1998) 137.
[10] Y. Lin, Z. Zhan, S.A. Barnett, Solid State Ionics 176 (2005) 1827.
[11] Y. Jiang, A.V. Virkar, J. Electrochem. Soc. 150 (2003) A942.
[12] E. Ramirez-Cabrera, A. Atkinson, D. Chadwick, Appl. Catal. B: Environ. 47 (2004) 127.
[13] O. Marina, M. Mogensen, Appl. Catal. A: Gen. 189 (1999) 117.
[14] Z. Zhan, S.A. Barnett, Science 308 (2005) 844.
[15] M. Krumpelt, D.-J. Liu, U.S. Patent Application Publication, Cont-in-part of U.S. Ser. no. 423,461, 2004, p. 18.